Published OnlineFirst November 6, 2020; DOI: 10.1158/1535-7163.MCT-20-0454

A Precision Medicine Drug Discovery Pipeline Identifies Combined CDK2 and 9 Inhibition as a Novel Therapeutic Strategy in Colorectal Cancer

Jason A. Somarelli[1], Roham Salman Roghani[1,2], Ali Sanjari Moghaddam[1,2], Beatrice C. Thomas[1], Gabrielle Rupprecht[1,2], Kathryn E. Ware[1], Erdem Altunel[1,2], John B. Mantyh[1,2], So Young Kim[3], Shannon J. McCall[4], Xiling Shen[2,5], Christopher R. Mantyh[6], and David S. Hsu[1,2]

ABSTRACT

Colorectal cancer is the third most common cancer in the United States and responsible for over 50,000 deaths each year. Therapeutic options for advanced colorectal cancer are limited, and there remains an unmet clinical need to identify new treatments for this deadly disease. To address this need, we developed a precision medicine pipeline that integrates high-throughput chemical screens with matched patient-derived cell lines and patient-derived xenografts (PDX) to identify new treatments for colorectal cancer. High-throughput screens of 2,100 compounds were performed across six low-passage, patient-derived colorectal cancer cell lines. These screens identified the CDK inhibitor drug class among the most effective cytotoxic compounds across six colorectal cancer lines. Among this class, combined targeting of CDK1, 2, and 9 was the most effective, with IC_{50}s ranging from 110 nmol/L to 1.2 μmol/L. Knockdown of CDK9 in the presence of a CDK2 inhibitor (CVT-313) showed that CDK9 knockdown acted synergistically with CDK2 inhibition. Mechanistically, dual CDK2/9 inhibition induced significant G_2–M arrest and anaphase catastrophe. Combined CDK2/9 inhibition *in vivo* synergistically reduced PDX tumor growth. Our precision medicine pipeline provides a robust screening and validation platform to identify promising new cancer therapies. Application of this platform to colorectal cancer pinpointed CDK2/9 dual inhibition as a novel combinatorial therapy to treat colorectal cancer.

Introduction

Colorectal cancer is the third most common cancer in the world, with approximately 150,000 new cases in the United States each year and the third leading cause of cancer-related deaths (1). At initial diagnosis, approximately 20% of patients will have distant metastasis, and another 25%–30% of patients with stage II/III disease will develop metastasis (2, 3). Currently, the use of chemotherapy in the metastatic setting can palliate symptoms and improve survival, but cannot cure patients. If left untreated, patients with colorectal cancer metastasis have an overall survival of just 6–9 months (4), but with combination therapy, survival can be improved to greater than 24 months (5, 6). However, despite these improvements, metastatic colorectal cancer remains an incurable and debilitating disease.

The concept of precision medicine is to apply the most effective therapeutic strategy to each patient at the right time to improve efficacy and minimize toxicity for patients. However, prior to the incorporation of new therapeutic agents in the clinical setting, these drugs must be assessed for their therapeutic potential in predictive preclinical models. Patient-derived models of cancer, such as cell lines, organoids, and patient-derived xenografts (PDX), are increasingly being accepted as "standard" preclinical models to facilitate the identification and development of new therapeutics. For example, large-scale drug screens of cancer patient–derived cell line panels have been used to identify sensitivity to a large number of potential therapeutics (7). Similarly, tumor organoid cultures from colorectal cancer specimens have also been used to perform drug screens (8), and colorectal cancer PDXs are being used to predict drug response (9) and identify novel drug combinations (10). Combinations of these patient-derived models of cancer are also being explored to develop precision medicine workflows for cancer care (11).

In this study, we developed a precision medicine strategy for patients with metastatic colorectal cancer. Specifically, we developed a series of patient-matched early-passage cell lines and PDXs to identify the most efficacious agents for metastatic colorectal cancer. In our pipeline, our early passage cell lines were first used to perform high-throughput drug screens across multiple cell lines to identify potential therapeutic targets, and the top targets were subsequently validated in matching PDXs. Using this approach, we identified the cyclin-dependent kinase (CDK) family as promising targets in the treatment of metastatic colorectal cancer. Further interrogation of this class of inhibitors in our screens revealed combined inhibition of CDK2 and CDK9 as the primary driver of efficacy.

Our findings suggest that the use of matched low-passage cell lines and PDXs is a useful platform to identify novel inhibitors. This platform led to the identification of dual CDK2/9 inhibition as a promising therapeutic strategy to treat metastatic colorectal cancer.

[1]Department of Medicine, Division of Medical Oncology, Duke University Medical Center, Durham, North Carolina. [2]Center for Genomics and Computational Biology, Duke University, Durham, North Carolina. [3]Duke Functional Genomics Core, Duke University, Durham, North Carolina. [4]Department of Pathology, Duke University, Durham, North Carolina. [5]Department of Biomedical Engineering, Duke University, Durham, North Carolina. [6]Department of Surgery, Duke University, Durham, North Carolina.

Note: Supplementary data for this article are available at Molecular Cancer Therapeutics Online (http://mct.aacrjournals.org/).

J.A. Somarelli and R.S. Roghani contributed equally to this article.

Corresponding Author: David S. Hsu, Duke University Medical Center, 3008 Snyderman Building, 905 S. LaSalle St., Durham, NC 27710. Phone: 919-684-1739; Fax: 919-660-0178; E-mail: shiaowen.hsu@duke.edu

Mol Cancer Ther 2020;19:2516–27

doi: 10.1158/1535-7163.MCT-20-0454

Published OnlineFirst November 6, 2020; DOI: 10.1158/1535-7163.MCT-20-0454

Materials and Methods

Development of PDX models of colorectal cancer

Patient tumor samples were collected in partnership with the Duke BioRepository & Precision Pathology Center at the time of the patient's surgical resection. Work was performed under a Duke Institutional Review Board (IRB)-approved protocol (Pro00002435). Development of PDXs was performed as described in our previous studies (10, 12). Briefly, surgically resected tumors were washed with phosphate-buffered saline (PBS) and minced to small (<2 mm^3) fragments. Tumor fragments were further dissociated with a tissue dissociation kit (gentleMACS Dissociator). Subsequently, 150 μL of homogenized tumor tissue suspensions (150 mg/mL concentration) were injected into the flanks of 8- to 10-week-old severe combined immunodeficient (SCID) mice (obtained from the Duke University Rodent Genetic and Breeding Core). Mice were monitored a minimum of thrice weekly. Upon identification of initial tumor appearance, tumor size was measured by digital calipers. When tumors reached 1 cm^2, tumors were harvested and used to create matched cell lines. All animal procedures were performed in accordance with the Duke University Institutional Animal Care and Use Committee.

Development of early-passage colorectal cancer cell lines

As described previously (10), colorectal cancer cell lines were generated from early-passage PDXs. After harvesting PDXs, homogenized single-cell solutions were prepared and grown in 10 cm^2 tissue culture dishes in the presence of complete cell culture media containing DMEM, 10% FBS, 100 IU/mL penicillin and 100 μg/mL streptomycin at 5% CO_2 and 37°C. To acquire pure cell lines for each PDX, a single colony of cancer cells was isolated within an O ring, trypsinized, and placed into 24-well plates. A total of six cell lines were established, including CRC057 (liver metastasis), CRC119 (liver metastasis), CRC16–159 (primary colon tumor), CRC240 (liver metastasis), CRC247 (liver metastasis), and CRC401 (primary rectal tumor). Cell lines were authenticated by the Duke University DNA Analysis Facility using polymorphic short tandem repeat (STR) genetic profiling (GenePrint 10 kit from Promega).

High-throughput chemical screens

High-throughput drug screens were performed in collaboration with the Duke University Functional Genomics Shared Resource. Briefly, each of 2,100 compounds from the BioActive small-molecule library (SelleckChem) was stamped in triplicate onto 384-well plates for a final concentration of 1 μmol/L using an Echo Acoustic Dispenser (Labcyte). Next, 500–1,000 cells per well was distributed using a Well mate (Thermo Fisher Scientific). Cells and compounds were incubated for three days, after which cell viability was assessed using the CellTiter-Glo Luminescent Cell Viability Assay (Promega) on a Clariostar plate reader (BMG Labtech). Percent killing was quantified using the formula 100 × (1-(average $CellTiterGlo^{drug}$/average $CellTiterGlo^{DMSO}$)) where the value average $CellTiterGlo^{DMSO}$ was the average DMSO CellTiterGlo value across each plate.

In vitro drug sensitivity assay

In vitro drug sensitivity assays were performed by treating each cell line with a CDK1/2/9 inhibitor (AZD5438), CDK9 inhibitor (LDC067), CDK2 inhibitor (CVT-313), or a CDK1 inhibitor (RO-3306). To do this, cells at 70%–80% confluency were plated into 96-well plates at 4,000 cells/well and incubated for 24 hours in drug-free media. After 24 hours of incubation, cells were treated with drug at a range of doses, starting from either 50 μmol/L or 100 μmol/L, depending on the cell line, with a serial dilution factor of three and a 10-point dose curve. A total of five replicates were included for each drug dose. Cells were incubated in the presence of drug for two days, after which the number of metabolically viable cells was estimated using CellTiter-Glo Luminescent Cell Viability Assay kit (Promega). All drugs were purchased from SelleckChem. All *in vitro* drug sensitivity assays were performed at least two independent times. The *in vitro* drug sensitivity assay results were reported as half maximal inhibitory concentration (IC_{50}).

Kaplan–Meier survival analysis

Data to create Kaplan–Meier curves were collected the Cancer Genome Atlas for colorectal adenocarcinoma (*COADREAD*). The UCSC Xena browser (13) was used to extract expression data for CDKs, pathologic stage, days to last fallow up and days to death data. Data was divided by median or quartiles, and GraphPad Prism software was used to draw Kaplan–Meier graphs.

Knockdown studies

From a 10 μmol/L working stock, 10 μL of nonsilencing or CDK9 siRNAs (Qiagen) were added to 1 mL of OptiMem (Sigma). In a separate tube, 20 μL of Lipofectamine RNAiMax (Thermo Fisher Scientific) was added to 1 mL of OptiMem. The two solutions were mixed and incubated at room temperature for 20 minutes. During this time, 1.5 mL of cell suspension (333,000 cells/mL) was plated into each well of a 6-well plate. After 20 minutes, 1 mL of the siRNA mixtures was added to each well of the plate and incubated overnight. The following day, cells were plated in a 96-well plate, while the media on the remaining wells was switched to normal DMEM supplemented with 10% FBS and 1% penicillin/streptomycin. After 24 hours, cells were incubated in triplicate in the presence of vehicle (dimethyl sulfoxide; DMSO) or a range of drug concentrations serially diluted 1:3 starting from 50 μmol/L. The dose curves were incubated for 48 hours, after which CellTiter-Glo (Promega) was added to the wells and imaged on a microplate reader (Molecular Devices). Results were uploaded to Prism, normalized to DMSO treated wells, and plotted using a 4-point nonlinear regression analysis.

Western blotting analysis

For knockdown validation, siRNA-treated cells were lysed in radioimmunoprecipitation assay lysis buffer supplemented with phosphatase and protease inhibitor (Thermo Fisher Scientific). The concentration of the protein lysates was determined using the BCA Protein Assay (Bio-Rad). A total of 50 μg of lysate was electrophoretically separated on 4%–20% SDS polyacrylamide gels using the Bio-Rad Miniprotean Tetra system and transferred to polyvinylidene difluoride membranes (Bio-Rad). Subsequent to blocking in StartingBlock T20 (Thermo Fisher Scientific), membranes were incubated with primary antibodies against CDK9 (Thermo Fisher Scientific; catalog number: MA5–14912) or β-actin (Santa Cruz Biotechnology), followed by the appropriate secondary antibodies at manufacturer-recommended dilutions. Blots were scanned and analyzed using a LI-COR Odyssey imaging system.

Cell-cycle arrest analysis

A total of 300,000 cells were plated in 6-well plates and incubated at 37 °C with 5% CO_2 until they reached approximately 60% confluence. Cells were treated with 0.1% DMSO or three times the IC_{50} dose of AZD5438 in full growth media. After 24 hours, 2×10^6 cells were harvested and washed twice with PBS, fixed in in 80% ethanol on ice for 30 minutes, washed twice more with PBS, and resuspended in cell staining buffer [0.1% Triton X-100, 0.1 mmol/L EDTA disodium,

Published OnlineFirst November 6, 2020; DOI: 10.1158/1535-7163.MCT-20-0454

50 μg/mL Rnase A and 50 ug/mL propidium iodide (PI) in PBS]. Flow cytometry was performed in conjunction with the Duke University Flow Cytometry Shared Resource.

Chromosomal stability assay

A total of 100,000 cells were plated in 6-well plates and incubated for 48 hours. Cells were treated for 16 hours as described for the cell-cycle analysis, after which, cells were fixed in 4% paraformaldehyde for 15 minutes and permeabilized for 30 minutes with 0.1% Triton-100X in PBS. Subsequent to blocking with normal goat serum, cells were treated with a 1:5,000 dilution of mouse anti α-tubulin antibody (Cell Signaling Technology) for 16 hours at 4°C, and stained with Hoechst dye (1:2,000; Thermo Fisher Scientific) and goat anti-mouse secondary antibody (1:5,000; LI-COR Biosciences). Cells were analyzed using an Olympus epifluorescence microscope at 400× total magnification. Cells were quantified from a total of 10 microscopic fields per treatment group.

In vivo studies

To evaluate the effect of CDK inhibition on CRC240 PDXs *in vivo*, homogenized PDX tissue–PBS suspension (150 μL at 150 mg/mL concentration) was subcutaneously injected into the right flanks of $n = 20$ male mice (JAX NOD.CB17-PrkdcSCID-J, 8–10 weeks) and randomized into four groups ($n = 5$ per group) to receive either vehicle (DMSO), CDK2 inhibitor (CVT-313), CDK9 inhibitor (LDC067), or the combination (CVT-313 + LDC067). Tumor volumes were measured regularly, and treatments were started when the tumor reached a volume of 250 mm^3. PDXs were treated with intraperitoneal injections of either CVT-313 (0.625 mg/kg/every other day), LDC000067 (5 mg/kg/every other day), CVT-313 + LDC067 (0.625 mg + 5 mg/kg/every other day, respectively) or vehicle (2% DMSO every other day). Both drugs were diluted in DMSO according to company protocol and further diluted in sterile pure water to reduce the DMSO concentration to less than 2%. Mice were examined regularly, and tumor volume was charted until endpoint of either maximal tumor size of 4,000 mm^3 or death for 14 days. All mice were euthanized after completion of experiment. Tumor sizes were measured using a digital Vernier caliper, and tumor volumes were estimated using the following formula: (length × $(width)^2$)/2.

Statistical analyses

All statistical analyses were performed in GraphPad Prism software. *t* tests (two groups) and ANOVA (three or more groups) with Tukey *post hoc* correction was used to compare differences between groups. A $P < 0.05$ was considered statistically significant.

Results

Development of PDXs and patient derived cell lines

In our previous work, we established a series of matched low-passage cell lines and patient-derived xenografts (PDX) to study the biology and genomics of colorectal cancer (10). These studies revealed

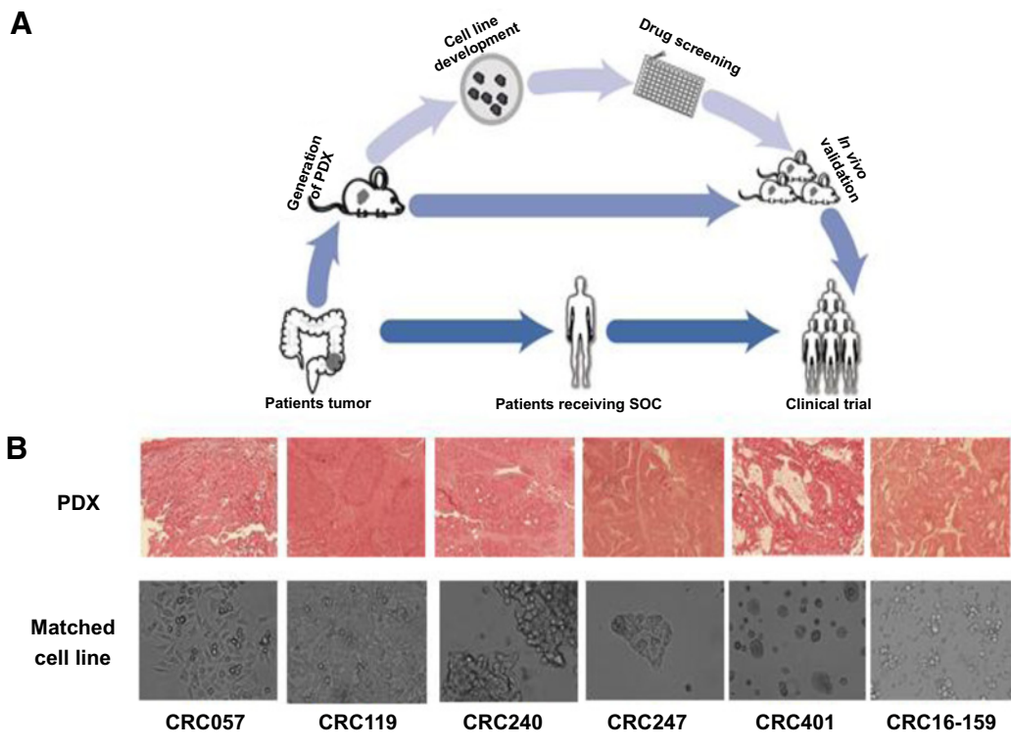

Figure 1.

A precision medicine pipeline for the treatment of colorectal cancer. **A,** To generate the precision medicine pipeline, colorectal cancer samples are processed and injected into immunodeficient mice to generate PDXs. Low-passage cell lines are generated from PDXs to perform high-throughput chemical screens and identify promising therapeutic targets and agents. Matched PDXs are then used to validate these candidate therapies. Validation in preclinical models and genomic studies allow for development of predictive biomarkers that can easily be integrated into clinical trials. **B,** Histologic features of the patient tumors (top), PDXs (middle), and matched PDX cell lines (bottom).

Published OnlineFirst November 6, 2020; DOI: 10.1158/1535-7163.MCT-20-0454

important parallels between patient-derived models and the tumors from which they were originally derived (10, 12, 14). Here, we sought to leverage these valuable patient-derived models to establish a precision medicine pipeline to identify and validate promising new therapies for colorectal cancer and other cancers. To do this, we capitalized on the unique strengths of each component of the pipeline, using the low-passage cell lines for high-throughput chemical screens and mechanistic studies then using the PDXs to validate efficacy for promising agents *in vivo* (**Fig. 1A**).

To implement our colorectal cancer precision medicine pipeline, we first developed patient-derived models of cancer including low passage cell lines and patient-derived xenografts (PDX). Samples were obtained from patients undergoing resection of their colorectal cancer (either metastatic or primary disease) at Duke University under an Institutional Review Board (IRB)- and Institutional Animal Care and Use Committee (IACUC)-approved protocol. For each patient, matching cell lines and PDXs (CRC057, CRC119, CRC240, CRC247, CRC401 and CRC16–159) were developed as described previously (12, 14) for this project. Patient demographics are described in **Table 1**, and **Fig. 1B** shows the histologic features of PDXs and the matching cell lines. There were two primary samples (CRC401 and CRC16–159) and four samples from colorectal cancer liver metastasis (CRC057, CRC119, CRC240, and CRC247; **Table 1**; **Fig. 1B**). Three samples were from patients self-reported to be of African ancestry (CRC119, CRC247, and CRC16–159) and three were from patients self-reported to be of European ancestry (CRC057, CRC240, and CRC401). There were four female patients (CRC057, CRC119, CRC401, and CRC16–159) and two male patients (CRC240 and CRC247). All were diagnosed with adenocarcinoma of the colon, with two found to be poorly differentiated (CRC240 and CRC401). One patient (CRC16–159) had a tumor with microsatellite instability that also had a BRAF mutation, and 4 had KRAS-mutated tumors (CRC057, CRC119, CRC248, and CRC401). Overall, this set of models represents a diverse population of colorectal cancer specimens.

High-throughput drug screening identifies cyclin-dependent kinase inhibitors as promising therapeutic agents in colorectal cancer

To identify potential therapeutic agents, a high-throughput chemical screen was performed using the BioActives compound library (SelleckChem). This library contains 2,100 compounds and is comprised of both FDA-approved and non-FDA–approved bioactive small molecules. The BioActives library is fully annotated by target and pathway, enabling interrogation of single agents, rational combination therapies, and efficacious targets or pathways. High-throughput screens were performed on six early-passage colorectal cancer cell lines (CRC057, CRC119, CRC16–159, CRC240, CRC 247, and CRC401; Supplementary Fig. S1). Overall, across the entire panel of drugs, CRC16–159 and CRC119 were most broadly sensitive while CRC247 and CRC401 were the most resistant (Supplementary Fig. S1A). In addition, the vast majority of drugs had no effect on colorectal cancer cells, with over 90% of compounds showing lower than 25% cytotoxicity among all six cell lines and only 7.9% ($n = 116$) of drugs with average cytotoxicity of more than 50% (Supplementary Fig. S1B). We next utilized the annotations available for the BioActives library to interrogate the pathways for which multiple drugs demonstrated efficacy. To pinpoint drugs with broad efficacy across multiple patient-derived models, we focused on compounds in which at least five out of six cell lines were inhibited by more than 50% (**Fig. 2A**). This analysis produced 94 compounds, and to further understand the targets and pathways that may potentially represent the most efficacious therapeutic strategies for colorectal cancer, the drugs were categorized by their mechanisms of action and pathway-level annotations. At the pathway level, drugs targeting histone deacetylases (HDAC), heat shock proteins (HSPs), the MEK pathway, the proteasome, PI3K/mTOR pathway, and cyclin-dependent kinases (CDK) had the highest average percent killing across the entire panel (**Fig. 2B**). Several of these pathways have been previously identified as promising targets for colorectal cancer, such as MEK (15, 16) and the PI3K/mTOR pathway (17–19), while others remain investigational, such as the CDKs (20, 21).

Although CDK inhibitors have been studied extensively in breast and other cancers and are currently considered standard-of-care therapy in breast cancer, their use in colorectal cancer remains investigational (22–25). To validate the utility of targeting CDKs in colorectal cancer, we first compared the efficacy of CDK inhibitors against other pathway-specific inhibitors studied in colorectal cancer, such as mTOR/PI3K inhibitors, STAT inhibitors, and Wnt/β-catenin inhibitors (**Fig. 2C**), as well as standard-of-care therapy in metastatic colorectal cancer, including oxaliplatin, irinotecan, 5-FU/Xeloda, lonsurf and regorafenib (**Fig. 2D**). These analyses revealed that, in general, CDK inhibitors have higher antitumor activity in comparison with other pathway-specific inhibitors and even many standard-of-care therapies.

CDKs are a protein family of 21 genes, several of which exhibit functional redundancies with other members of the gene family (26). As such, inhibition of a single CDK could be compensated for by others, especially in the context of the ever-evolving landscape of metastatic colorectal cancer. Therefore, it was not surprising to find that almost all potent CDK inhibitors target multiple CDKs. We

Table 1. Patient demographics are described in Table 1.

Sample ID	Gender	Race	Histology	Grade	Microsatellite status	KRAS	BRAF	Site of tissue
CRC057	F	W	Adenocarcinoma	Moderately differentiated	MSS	G12C	WT	Liver
CRC119	F	AA	Adenocarcinoma	Moderately differentiated	MSS	G12V	WT	Liver
CRC240	M	W	Adenocarcinoma	Poorly differentiated	MSS	WT	WT	Liver
CRC247	M	AA	Adenocarcinoma	Moderately differentiated	MSS	G12D	WT	Liver
CRC401	F	W	Adenocarcinoma	Poorly differentiated	MSS	G12D	WT	Rectal
CRC16–159	F	AA	Adenocarcinoma	Moderately differentiated	MSI	WT	V600E	Colon

Published OnlineFirst November 6, 2020; DOI: 10.1158/1535-7163.MCT-20-0454

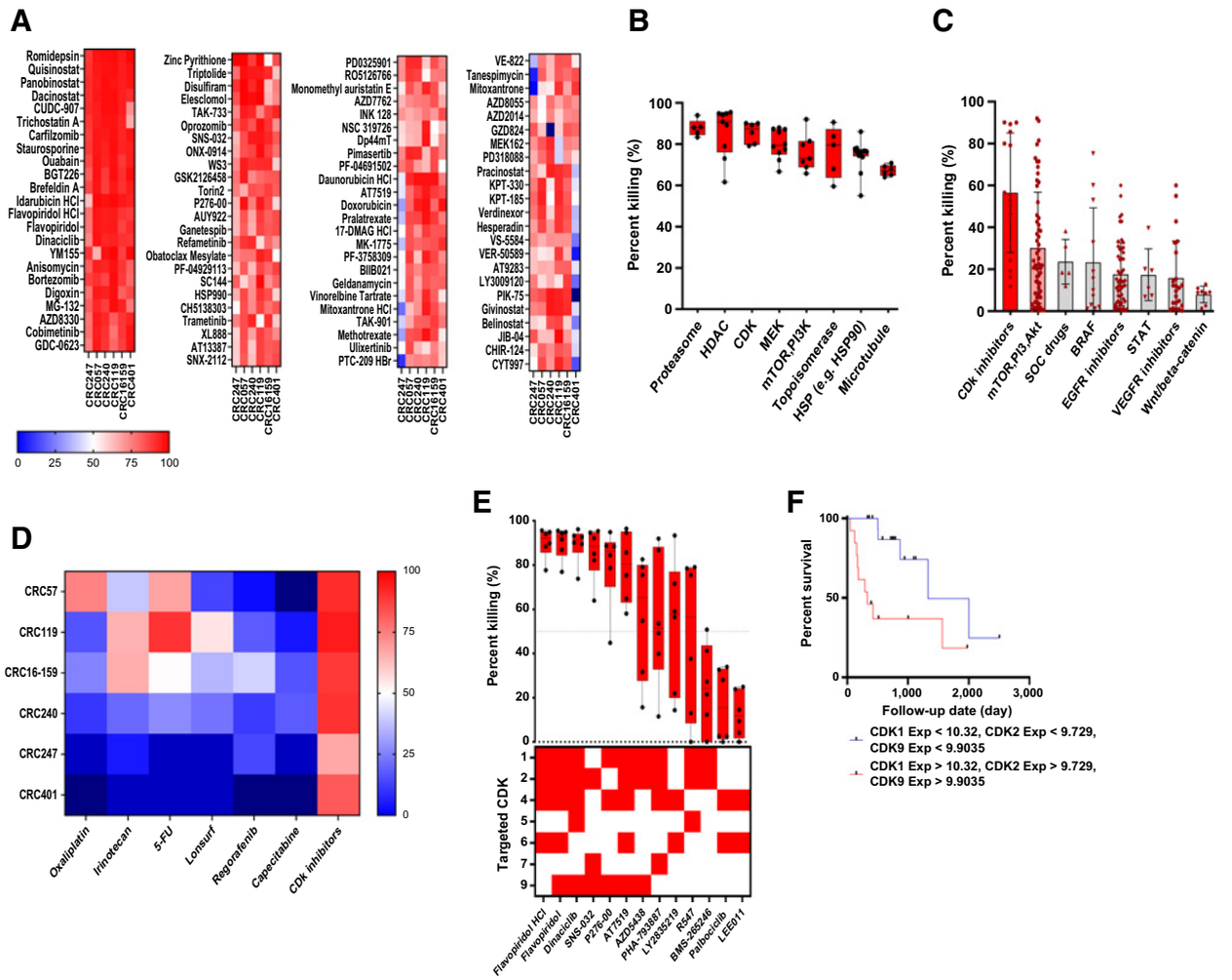

Figure 2.

Patient-derived models to identify therapeutic agents in colorectal cancer. **A,** High-throughput drug screen results for six early-passage colorectal cancer cell lines identified compounds ($n = 94$) for which at least five out of six cell line showed >50% inhibition. **B,** The proteasome, histone deacetylases (HDACs), cyclin-dependent kinases (CDKs), the MEK pathway, PI3K/mTOR pathway, topoisomerase, HSPs, and microtubule involved pathways had the highest average percent killing across the entire cell line panel. Each dot represents a single compound in each pathway (lines represent the median; boxes represent the 25th–75th percentile; whiskers represent the minimum and maximum values). **C,** CDK inhibitors had the highest antitumor activity compared with other signaling pathway inhibitors. Each dot represents a single compound with the mean and standard deviation shown for each group. **D,** A heatmap comparing CDK inhibitors to standard-of-care drugs in each cell line. **E,** CDK 1,2 and 9 are the most repetitive targets among the most effective CDK inhibitors for all six cell lines. CDK inhibitors and their targets are sorted from highest to lowest percent killing. Targeted CDKs are depicted by red squares for each compound. **F,** Kaplan–Meier gene expression analysis shows that combined increased expression of CDK1,2 and 9, confer a poorer prognosis in colorectal cancer (stages IV); $P = 0.005$. Samples are divided into groups based on the median expression value for the cohort.

therefore sought to determine the CDK combination with the highest efficacy. To do this, the CDK inhibitors and their targets were sorted from highest to lowest percent killing (**Fig. 2E**). These analyses revealed that drugs targeting combinations of CDK 1, 2, and 9 were among the most potent CDK inhibitors across the six patient-derived cell lines. Both CDK 1 and 2 are involved in cell-cycle regulation: CDK1 is involved in G_2–M progression while CDK2 promotes G_1 and S-phase progression (27, 28). CDK9, on the other hand, serves an independent function in transcription and can inhibit cancer cell proliferation beyond disruption of the cell cycle (29). As studies have shown mechanistic synergy between these classes of CDKs (30, 31), we concluded that the combination of CDK1, 2, and 9 may be an effective combination strategy in the treatment of metastatic colorectal cancer.

Consistent with our drug screen results, which pinpointed CDK1, 2, and 9 as being novel targets for colorectal cancer, analysis of CDK1, 2, and 9 expression in colorectal cancer from The Cancer Genome Atlas suggests that, while the individual expression of most of these CDKs is not a prognostic marker for early-stage disease (stages I–III, Supplementary Fig. 2), increased expression of these three CDKs in combination is correlated with poor prognosis for overall survival in advanced (stage IV) colorectal cancer (**Fig. 2F**), reinforcing the potential utility of targeting these CDKs in colorectal cancer.

Published OnlineFirst November 6, 2020; DOI: 10.1158/1535-7163.MCT-20-0454

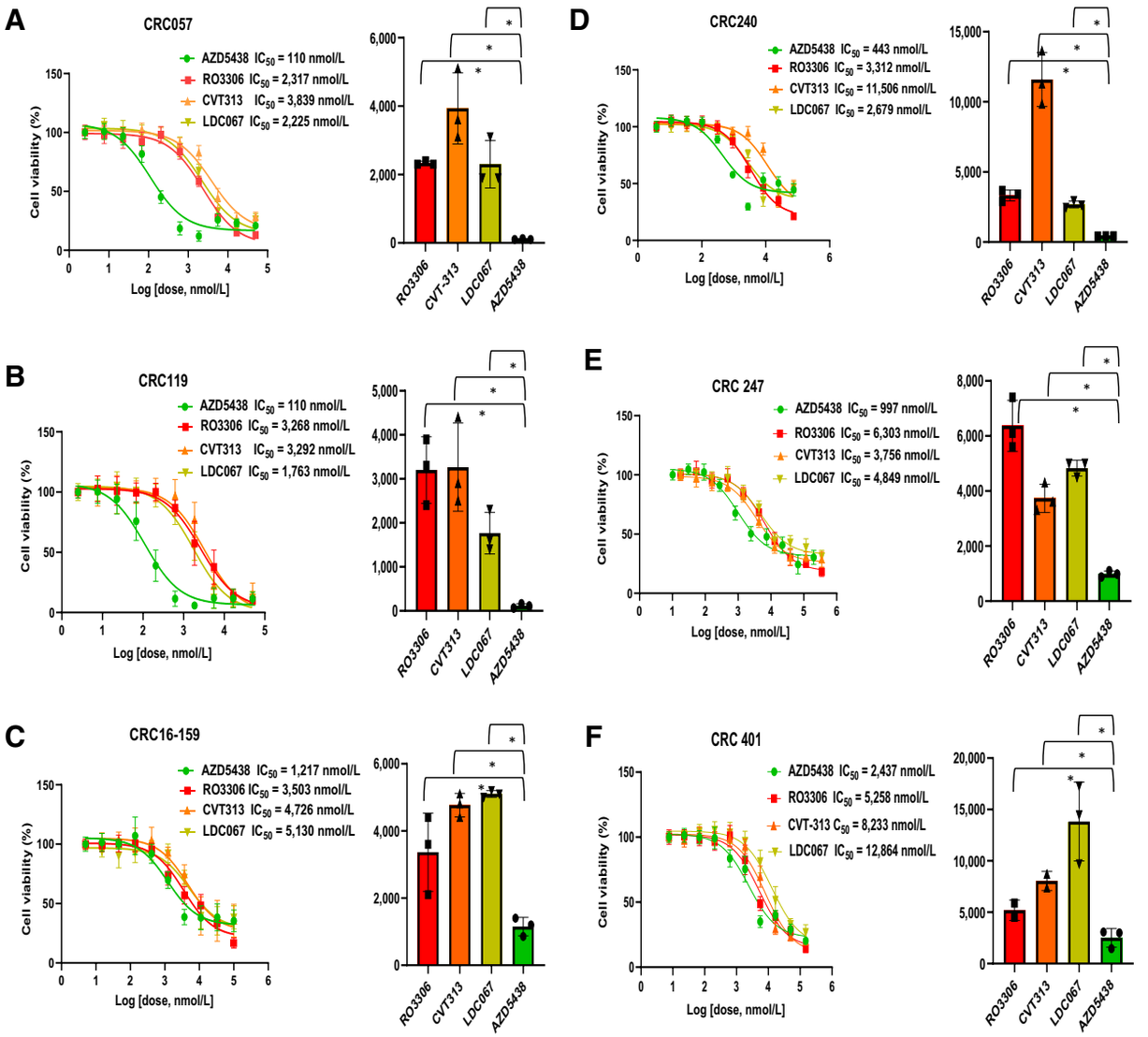

Figure 3.

Drug sensitivity studies validate the synergistic efficacy of CDK1/2/9 inhibition. Drug sensitivity studies were performed on six early passage colorectal cancer cell lines [CRC057 (**A**), CRC119 (**B**), CRC16–159 (**C**), CRC240 (**D**), CRC 247 (**E**) and CRC401 (**F**)]. Across all cell lines, IC_{50} of AZD5438 (CDK1, 2, and 9 inhibitor) were lower than RO-3306 (CDK1 inhibitor), CVT-313 (CKD2 inhibitor), and LDC000067 (CDK9 inhibitor); $^*P < 0.01$.

Combining CDK1/2/9 inhibition significantly enhances the antitumor effect *in vitro*

Next, to determine the efficacy of CDK1, 2, and 9 inhibition on colorectal cancer both as single agents and in combination, we performed IC_{50} dose–response curves on our early-passage colorectal cancer cell lines (CRC057, CRC119, CRC16–159, CRC240, CRC 247, and CRC401) with a CDK1 inhibitor (RO-3306), CDK2 inhibitor (CVT-313), CDK9 inhibitor (LDC067), and a CDK1,2,9 inhibitor (AZD5438; **Fig. 3A**–**F**). Single-agent inhibition by RO-336, CVT-313 or LDC067 showed minimal efficacy, with estimated IC_{50} values ranging from 1.7 μmol/L (CDK9 inhibitor, LDC067) to 7.6 μmol/L (CDK2 inhibitor, CVT-313). In contrast, we observed that the CDK1/2/9 inhibitor, AZD5438, had significantly lower IC_{50} values ranging from 110 nmol/L to 3 μmol/L ($P < 0.001$). Specifically, CRC057 (**Fig. 3A**) and CRC119 (**Fig. 3B**), both with IC_{50} of 110 nmol/L, were found to be most sensitive to AZD5438, whereas CRC16–159 (**Fig. 3C**), with IC_{50} of 1.2 μmol/L, and CRC401 (**Fig. 3F**) with an IC_{50} of 3.0 μmol/L, were found to be the most resistant. Together, these results showed that combined CDK1, 2, and 9 inhibition could be an efficacious treatment strategy for patients with metastatic colorectal cancer.

CDK1/2/9 inhibition induces cell-cycle arrest and anaphase catastrophe in colorectal cancer cell lines

Inhibition of CDK 1 or 2 induces potent cell-cycle arrest (32). Therefore, to confirm target-specificity of AZD5438, we analyzed cell-cycle progression for CRC057, CRC119, CRC16–159, and CRC240 cells treated with vehicle or AZD5438 (**Fig. 4**). Specifically, CDK2 promotes S-phase progression while CDK1 promotes G_2 progression and entry into mitosis (33, 34). Consistent with the known

Published OnlineFirst November 6, 2020; DOI: 10.1158/1535-7163.MCT-20-0454

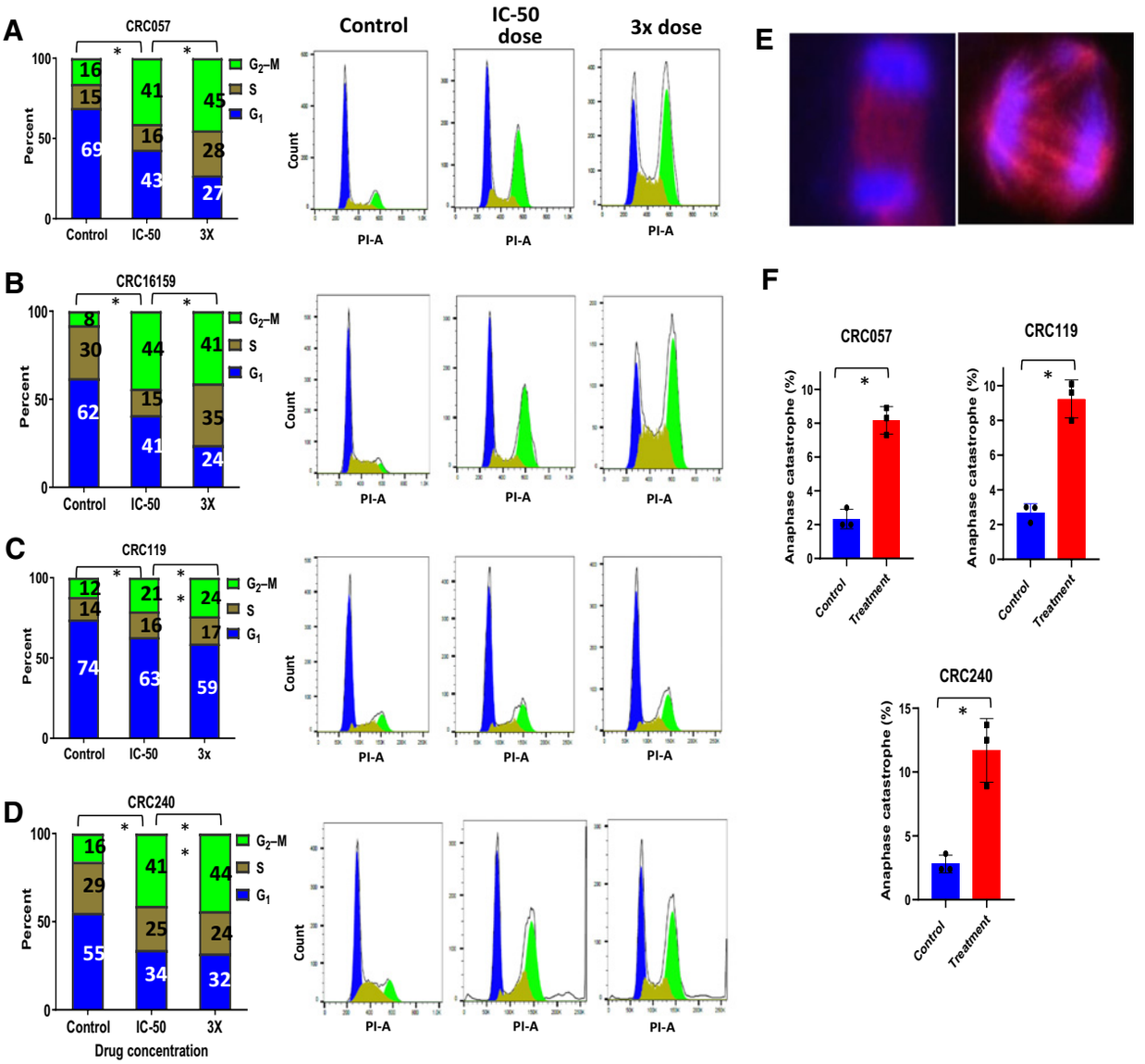

Figure 4.

AZD5438 induces cell-cycle arrest and anaphase catastrophe in colorectal cancer cells. Cell-cycle analysis was performed to determine whether AZD5438 inhibits proliferation of colorectal cancer cells via disruption of the cell cycle. Cells were treated with vehicle (0.1% DMSO), the IC_{50} dose of AZD5438, or three times the IC_{50} dose of AZD5438 for 24 hours, stained with propidium iodide, and analyzed by flow cytometry. AZD5438 interfered with the cell cycle by significantly increasing arrest in S and G_2–M in a dose-dependent manner in CRC057 (**A**) and CRC16–159 (**B**). A significant increase in S and G_2–M arrest was observed in CRC119 (**C**) and CRC240 cells (**D**; *, $P < 0.001$, **, $P > 0.05$). **E,** CRC057 cells treated with vehicle (DMSO) exhibit normal bipolar mitosis (left) while treatment with AZD5438 led to anaphase catastrophe, with cells exhibiting multipolar mitosis (right). **F,** Quantification of anaphase catastrophe in vehicle- and AZD5438-treated cells (*, $P < 0.05$).

mechanisms of CDK1 and 2 inhibition, treatment of CRC057 and CRC16–159 with AZD5438 led to a significant, dose-dependent increase in S and G_2–M phase arrest (**Fig. 4A** and **B**). There was also a significant increase in S and G_2–M phase arrest in CRC119 and CRC240 upon treatment with AZD5438 (**Fig. 4C** and **D**). These analyses confirm target specificity for AZD5428 in our cell lines.

To further examine the mechanism of action of AZD5438 in promoting cell death, we tested whether AZD5438 was inducing anaphase catastrophe. Anaphase catastrophe is a pro-apoptotic pathway that has been shown to be the mechanism of action upon CDK2 inhibition (35). Because the inhibitory effect of AZD5438 is, in part, due to CDK2 inhibition, we investigated whether the same antitumor activity could be seen in our colorectal cancer cell lines. To do this, CRC057 cells were treated with two different doses of AZD5438 (the IC_{50} dose and three times the IC_{50}) for 12 hours. Treatment with AZD5438 induced anaphase catastrophe as observed by multipolar spindles during anaphase (**Fig. 4E**). AZD5438 treatment led to a significant increase in the number of cells undergoing anaphase

Published OnlineFirst November 6, 2020; DOI: 10.1158/1535-7163.MCT-20-0454

catastrophe in the treatment group compared with vehicle-treated control cells (**Fig. 4F**).

RNAi-mediated knockdown of CDK9 pinpoints combined CDK2/9 inhibition as the most effective combination therapy

Our data suggest combined inhibition of CDKs 1, 2, and 9 outperforms single-agent inhibition of any one of these CDKs in isolation. However, because CDK1 and 2 have partially-redundant functions in cell-cycle regulation, it was unclear which of the CDKs is responsible for the synergistic activity of the CDK1/2/9 inhibitor, AZD5438. To further dissect the relative importance of CDK1 or CDK2 inhibition in combination with CDK9 inhibition we performed siRNA-mediated knockdowns of CDK9 in combination with inhibition of either CDK1 or 2. We first assessed the efficacy of three independent siRNAs targeting CDK9 by western blots in CRC057 (**Fig. 5A**), CRC16–159 (**Fig. 5B**), and CRC119 (**Fig. 5C**). Among these three siRNAs, siRNA_8 provided the most complete knockdown of CDK9 all three cell lines (**Fig. 5A–C**). We next performed siRNA-mediated knockdowns of CDK9 with or without drug-mediated inhibition of CDK1 (RO-3306) or CDK2 (CVT-313). Interestingly, while there was no synergistic effect between CDK9 knockdown and treatment with the CDK1 inhibitor, R0–3306 (positive delta score) (**Fig. 5D–F**), we observed a synergistic effect of CDK9 knockdown upon CDK2 inhibition (CVT-313) for all cell lines (**Fig. 5G–I**). These results suggest that CDK1 inhibition is dispensable for the efficacy of AZD5438 and that the mechanism of action for AZD5438 is likely due predominantly to combined CDK2 and CDK9 inhibition.

Dual inhibition of CDK2/9 synergistically inhibits tumor growth compared with single-agent CDK inhibitors *in vivo*

To validate the efficacy of dual inhibition of CDK2 and 9, we tested whether combined inhibition of CDK2 and 9 was capable of reducing tumor growth *in vivo*. To do this, matched PDXs of CRC240 were treated with either vehicle (DMSO), the CDK2 inhibitor, CVT-313, (5 mg/kg), the CDK9 inhibitor, LDC000067 (0.625 mg/kg) or in combination. **Figure 6A** shows that treatment with CVT-313 or LDC000067 resulted in minimal tumor growth inhibition; however, consistent with our *in vitro* observations using both small molecules and siRNAs, the combined inhibition of both CDK2 and 9 led to synergistic and significant tumor growth inhibition. Importantly, no additional toxicities, such as weight loss, diarrhea, limb weakness, anxiety/restlessness, or hair loss, were observed in the mice treated with the combination therapy (**Fig. 6B**). Collectively, these *in vitro* and *in vivo* results indicate that dual CDK2 and 9 inhibition could be a promising and tolerable therapy for patients with metastatic colorectal cancer.

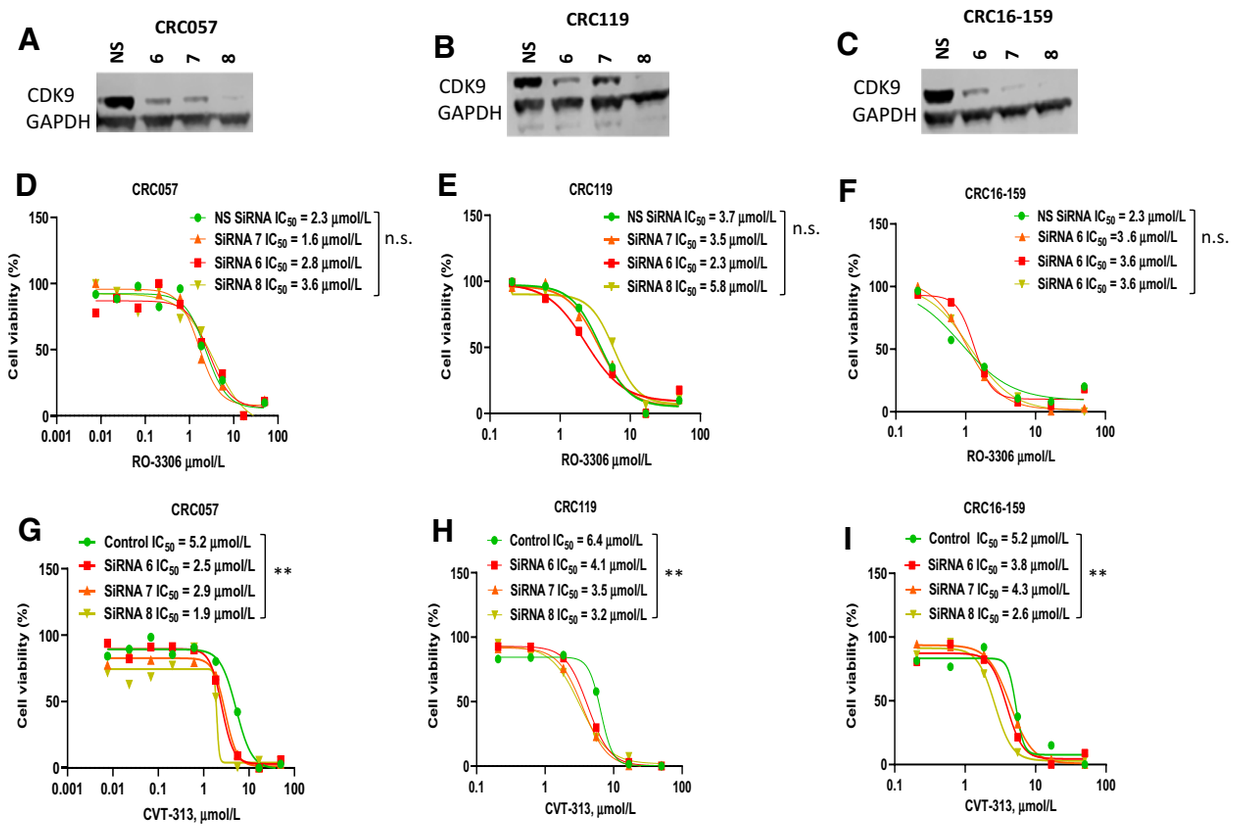

Figure 5.
RNAi-mediated knockdown of CDK9 sensitizes colorectal cancer cells to CDK2 inhibition. **A–C,** Validation of three independent siRNAs targeting CDK9 (6, 7, 8) were used for CDK9 knockdown by Western blotting in CRC057 (**A**), CRC119 (**B**), and CRC16–159 (**C**). **D–F,** The siRNA-mediated knockdown of CDK9 with siRNA 6,7 and 8 showed no change in IC_{50} for CRC057 (**D**), CRC119 (**E**), and CRC16–159 (**F**). **G–I,** siRNA knockdown of CDK9 with siCDK9_6, 7, and 8 showed synergy with CDK2 inhibition, with significantly decreased IC_{50} for CRC057 (**G**), CRC119 (**H**), and CRC16–159 (**I**); **, $P < 0.05$.

Published OnlineFirst November 6, 2020; DOI: 10.1158/1535-7163.MCT-20-0454

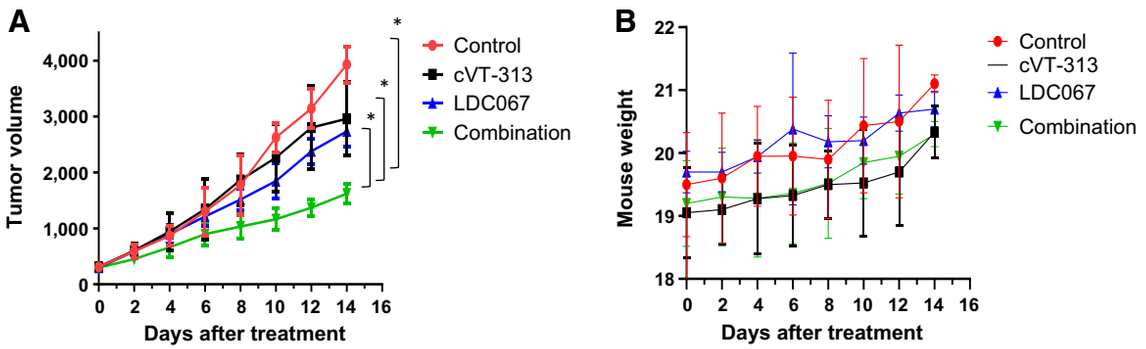

Figure 6.

Dual inhibition of CDK2/9 synergistically inhibits tumor growth in colorectal cancer PDXs. **A,** CRC240 PDXs were treated with either vehicle (DMSO), CVT-313 (CDK2 inhibitor), LDC000067 (CDK9 inhibitor) or combined CDK2 and CDK9 inhibitors. After 14 days of treatment, combination of CVT-313 and LDC000067 resulted in significant tumor growth inhibition as compared to CVT-313 or LDC000067 alone; *, $P < 0.05$. **B,** Mice showed no difference in weight between all four groups during the course of study; $P > 0.05$.

Discussion

Patient-derived models of cancer, such as early passage cell lines, patient-derived organoids, and PDXs are being accepted as efficient tools for the development of the cancer therapeutics and development of precision medicine pipelines (36, 37). Specifically, morphologic and molecular similarity between these models and the original patient tumors facilitates the evaluation of anticancer drug responses and the identification of mechanisms of resistance. Indeed, previous studies have demonstrated that PDXs can recapitulate the patient response to therapy (38, 39) and major efforts by both commercial and academic institutions are being developed to determine how patient-derived models of cancer can be best used to guide patient care. In our study, we have developed a novel precision medicine strategy for patients with colorectal cancer using matched early-passage cell lines and PDXs. We coupled these matched patient-derived models with high-throughput drug screens as a reliable means to identify (i) response to standard-of-care agents, (ii) patient specific target and pathway vulnerabilities, (iii) effective single-agent therapies, and (iv) rational combination therapies. These analyses led to the discovery of a novel combination of cyclin-dependent kinases (CDK2/9) as a treatment of colorectal cancer. Although a small dataset, we feel that this combination is potentially applicable across the general colorectal cancer population as **Table 1** showed that our samples consisted of males and females, European and African ancestry, mostly MSS tumors, but contained both KRAS WT and mutant samples, although it must be noted that one KRAS WT sample (CRC16–159) had a BRAF-mutant tumor. Indeed, the CDK2/9 combination was effective even in CRC-247 and CRC-401, both of which were broadly resistant to standard-of-care agents and were among the most resistant in the drug screen (**Fig. 2**). While the mechanisms of resistance to standard-of-care agents in these lines are unknown, both of these lines harbor a KRAS G12D mutation, which has been shown to promote therapy resistance in non–small cell lung cancer (40, 41). It is also worth noting other cell lines in the screen were also KRAS mutant, suggesting additional mechanisms of resistance in CRC-247 and CRC-401.

There has been considerable progress in our understanding about specific function of CDKs, which are involved in cell-cycle regulation and transcription. CDKs can be divided into two subgroups that directly or indirectly regulate the cell cycle, including CDKs1–6, 11 and 14–18, or transcription, including CDKs7–13, 19, and 20 (42). CDK1, CDK2, CDK4, and CDK6 and their associated Cyclins (A, B, D, and E) are considered fundamental cell-cycle regulators. CDK 2, 4, and 6 promote expression of genes essential for G_1 completion and progression through S-phase, while CDK 1 promotes G_2 progression and entry into mitosis (28). In contrast, CDK7/cyclin H and CDK9/cyclin T promote phosphorylation of the carboxy-terminal domain of RNA polymerase II, facilitating initiation and elongation of RNA transcription (28).

CDKs are best known for their remedial effect in breast cancer therapy, as FDA has approved three CDK4/6 inhibitors, including palbociclib, ribociclib, and abemaciclib, for the treatment of hormone receptor–positive and HER2-negative breast cancer (23–26). Although clinical benefit of other combinations of CDK inhibitors in various cancers has been studied in clinical trials (43–46), concerns have always been raised in terms of toxicity and tolerability (47). Unfortunately, few studies evaluating CDKs in colorectal cancer have been performed; however, these have shown minimal efficacy in colorectal cancer (48) and overall, the efficacy of CDK inhibitors in colorectal cancer remains unknown.

Similar to clinical trials in colorectal cancer that showed limited activity for single-agent CDKs, our data also suggest minimal activity for any of the CDKs as single agents. However, we observed significantly improved efficacy as combinatorial therapy. This is in agreement with studies that showed flavopiridol (CDK1, 2, 4 and 9 inhibitor) had promising antitumor activity in colorectal cancer xenografts (49). However, flavopiridol showed no activity in a phase II study in advanced colorectal cancer when used as a single agent (50). This lack of activity of flavopiriol was due to its toxicity in humans and the inability to achieve a therapeutic dose. Therefore, in our study we attempted to determine the minimal combination of CDK inhibition needed, while minimizing the toxicity to determine the most efficacious combination. The results of our study suggested that the combination of CDK2/9 inhibition, which targets both the cell cycle and transcription, is potentially the most optimal and minimal combination of CDK inhibition needed for the treatment of colorectal cancer.

Mechanistically, we showed that dual CDK2/9 inhibition led to cell cycle arrest and anaphase catastrophe. The degree of cell cycle arrest did not correlate with the degree of sensitivity to CDK2/9 inhibition, which may be due to the fact that CDK2 and CDK9 play

different functional roles, with CDK2 inhibition inducing cell-cycle arrest (51, 52), and CDK9 inhibition preventing transcription elongation (53). In addition to cell-cycle arrest, CDK2/9 inhibition also induced anaphase catastrophe. This is consistent with a previous study showing that the combination of CKD2/9 inhibition by CCT068127 exhibited antiproliferative activity by decreasing retinoblastoma protein (RB1) phosphorylation, reducing phosphorylation of RNA polymerase II, and inducing cell-cycle arrest and apoptosis in colorectal cancer and melanoma cell lines (54). Given that similar results were also observed in lung cancer (55), this suggests that targeting these two independent pathways of CDK inhibition could have synergistic effects in several cancers. The presence of supernumerary centrosomes is a common characteristic of many cancers (56). Normally, an increased centrosome number would lead to multipolar cell division and trigger cell death. Cancer cells overcome this problem by active clustering of supernumerary centrosomes at two poles, which ensures bipolar mitosis (57, 58). CDK2 inhibition has been shown to antagonize supernumerary centrosome clustering in lung cancer, which can lead to multipolar cell division and subsequent apoptosis (59, 35). Consistence with these observations, our data showed that CDK2 inhibition led to anaphase catastrophe in colorectal cancer cells.

However, as described above, a major concern of combinatorial CDK inhibition and potentially the combination of CDK2/9 inhibition is drug toxicity. Despite their efficacy, common adverse effects of CDK inhibitors include hematologic abnormalities, fatigue, and gastrointestinal symptoms, such as diarrhea, which can limit their clinical use. However, as our *vivo* PDX study showed that combined CDK2/9 inhibition acted synergistically, we were able to reduce the dose of both CDK2 and 9 inhibitors while maintaining improved efficacy and simultaneously minimizing drug toxicity. These encouraging properties of the CDK2/9 combination *in vivo* will allow us to further explore this combination as a viable clinical combination.

Finally, our models will also now allow us to study additional therapies that can be combined with CDK inhibitors to improve efficacy and overcome resistance both *in vitro* and *in vivo*. Indeed, studies have shown that CDK inhibitors can enhance apoptosis when combined with chemotherapy to overcome resistance in various cancers, including colorectal cancer (60, 61). Other studies have shown that potentiation of the p53 tumor suppressor by 5-fluorouracil had a synergic killing effect with a CDK7 inhibitor in colorectal cancer (62). Similarly, the $BRAF^{V600E}$ mutation in colorectal cancer is associated with therapeutic resistance secondary to reactivation of MEK/ERK signaling cascade, and Zhang and colleagues, showed that dual inhibition of multiple CDKs by dinaciclib (CDK1, 2, 5, 9 inhibitors) with MEK inhibition by cobimetinib (MEK inhibitor) can overcome resistance in BRAF-mutant colorectal cancer (63).

One limitation of the use of matched patient-derived cell lines and PDXs is the considerable time and resources needed to develop and apply these systems to drug discovery efforts. To address these limitations, researchers have turned to organoid systems that recapitulate the biology of patient tumors. These systems have been developed across a range of solid tumors, including colorectal cancer (8), pancreatic cancer (64), prostate cancer (65), liver cancer (66), breast cancer (67), and lung cancer (68). Advances in organoid culture technology have the potential to substantially increase the speed with which novel candidate therapies can be identified and translated into real-time clinical decision-making (reviewed in Kondo and colleagues; ref. 69).

In summary, the generation of our colorectal cancer precision medicine pipeline provides a robust platform to identify and validate potential new therapies with several advantages. First, a standardized workflow that combines matched patient-derived cell lines and PDXs provides maximal benefit by enabling a rapid screening and mechanistic validation tool. Second, capitalizing on the matched *in vivo* models facilitates validation of candidate therapies and mechanisms of response/resistance in matched PDXs *in vivo*. Studies from these models will pave the way to more rapidly identify, characterize, and validate new drugs for translation into the clinic.

Authors' Disclosures

S.J. McCall reports other from AstraZeneca (consultant) outside the submitted work. D.S. Hsu reports grants from NIH during the conduct of the study. No disclosures were reported by the other authors.

Authors' Contributions

J.A. Somarelli: Conceptualization, formal analysis, supervision, writing-original draft, writing-review and editing. **R.S. Roghani:** Resources, validation, investigation, writing-original draft, writing-review and editing. **A.S. Moghaddam:** Formal analysis, investigation, writing-review and editing. **B.C. Thomas:** Formal analysis, investigation, visualization, writing-review and editing. **G. Rupprecht:** Investigation, visualization, writing-review and editing. **K.E. Ware:** Supervision, investigation, writing-review and editing. **E. Altunel:** Investigation, writing-review and editing. **J.B. Mantyh:** Investigation. **S.Y. Kim:** Resources, formal analysis, investigation, writing-review and editing. **S.J. McCall:** Resources, writing-review and editing. **X. Shen:** Resources, writing-review and editing. **C.R. Mantyh:** Resources, writing-review and editing. **D.S. Hsu:** Conceptualization, resources, supervision, funding acquisition, investigation, writing-original draft, writing-review and editing.

Acknowledgments

We acknowledge the Duke BioRepository & Precision Pathology Center (BRPC, a shared resource of the Duke University School of Medicine and Duke Cancer Institute) for their regulatory and technical assistance in the procurement of the patient samples utilized in this study. The BRPC is supported by the P30 Cancer Center Support Grant (P30 CA014236). This work was supported, in part, by P30 CA014236 (NIH, Bethesda, MD).

The costs of publication of this article were defrayed in part by the payment of page charges. This article must therefore be hereby marked *advertisement* in accordance with 18 U.S.C. Section 1734 solely to indicate this fact.

Received June 3, 2020; revised August 15, 2020; accepted September 28, 2020; published first November 6, 2020.

References

1. Siegel RL, Miller KD, Jemal A. Cancer Statistics, 2017. CA Cancer J Clin 2017;67:7–30.
2. André T, Bensmaine MA, Louvet C, François E, Lucas V, Desseigne F, et al. Multicenter phase II study of bimonthly high-dose leucovorin, fluorouracil infusion, and oxaliplatin for metastatic colorectal cancer resistant to the same leucovorin and fluorouracil regimen. J Clin Oncol 1999;17:3560–8.
3. August DA, Sugarbaker PH, Ottow RT, Gianola FJ, Schneider PD. Hepatic resection of colorectal metastases. Influence of clinical factors and adjuvant intraperitoneal 5-fluorouracil via Tenckhoff catheter on survival. Ann Surg 1985;201:210–8.
4. Stangl R, Altendorf-Hofmann A, Charnley RM, Scheele J. Factors influencing the natural history of colorectal liver metastases. Lancet 1994;343:1405–10.
5. Hurwitz H, Fehrenbacher L, Novotny W, Cartwright T, Hainsworth J, Heim W, et al. Bevacizumab plus irinotecan, fluorouracil, and leucovorin for metastatic colorectal cancer. N Engl J Med 2004;350:2335–42.

6. Tournigand C, André T, Achille E, Lledo G, Flesh M, Mery-Mignard D, et al. FOLFIRI followed by FOLFOX6 or the reverse sequence in advanced colorectal cancer: a randomized GERCOR study. J Clin Oncol 2004;22: 229–37.
7. Barretina J, Caponigro G, Stransky N, Venkatesan K, Margolin AA, Kim S, et al. The cancer cell line encyclopedia enables predictive modelling of anticancer drug sensitivity. Nature 2012;483:603–7.
8. van de Wetering M, Francies HE, Francis JM, Bounova G, Iorio F, Pronk A, et al. Prospective derivation of a living organoid biobank of colorectal cancer patients. Cell 2015;161:933–45.
9. Gao H, Korn JM, Ferretti S, Monahan JE, Wang Y, Singh M, et al. High-throughput screening using patient-derived tumor xenografts to predict clinical trial drug response. Nat Med 2015;21:1318–25.
10. Lu M, Zessin AS, Glover W, Hsu DS. Activation of the mTOR pathway by oxaliplatin in the treatment of colorectal cancer liver metastasis. PLoS One 2017; 12:e0169439.
11. Pauli C, Hopkins BD, Prandi D, Shaw R, Fedrizzi T, Sboner A, et al. Personalized in vitro and in vivo cancer models to guide precision medicine. Cancer Discov 2017;7:462–77.
12. Uronis JM, Osada T, McCall S, Yang XYi, Mantyh C, Morse MA, et al. Histological and molecular evaluation of patient-derived colorectal cancer explants. PLoS One 2012;7:e38422.
13. Goldman M, Craft B, Brooks A, Zhu J, Haussler D. The UCSC Xena Platform for cancer genomics data visualization and interpretation. 2018.
14. Kim MK, Osada T, Barry WT, Yang XY, Freedman JA, Tsamis KA, et al. Characterization of an oxaliplatin sensitivity predictor in a preclinical murine model of colorectal cancer. Mol Cancer Ther 2012;11:1500–9.
15. Gong S, Xu D, Zhu J, Zou F, Peng R. Efficacy of the MEK inhibitor cobimetinib and its potential application to colorectal cancer cells. Cell Physiol Biochem 2018; 47:680–93.
16. Krishnamurthy A, Dasari A, Noonan AM, Mehnert JM, Lockhart AC, Leong S, et al. Phase Ib results of the rational combination of selumetinib and cyclosporin A in advanced solid tumors with an expansion cohort in metastatic colorectal cancer. Cancer Res 2018;78:5398–407.
17. Foley TM, Payne SN, Pasch CA, Yueh AE, Van De Hey DR, Korkos DP, et al. Dual PI3K/mTOR inhibition in colorectal cancers with APC and PIK3CA mutations. Mol Cancer Res 2017;15:317–27.
18. Narayanankutty A. PI3K/Akt/mTOR pathway as a therapeutic target for colorectal cancer: a review of preclinical and clinical evidence. Curr Drug Targets 2019;20:1217–26.
19. Ponnurangam S, Standing D, Rangarajan P, Subramaniam D. Tandutinib inhibits the Akt/mTOR signaling pathway to inhibit colon cancer growth. Mol Cancer Ther 2013;12:598–609.
20. Robb CM, Kour S, Contreras JI, Agarwal E, Barger CJ, Rana S, et al. Characterization of CDK(5) inhibitor, 20–223 (aka CP668863) for colorectal cancer therapy. Oncotarget 2018;9:5216–32.
21. Sankaranarayanan R, Valiveti C, Kumar D, Van slambrouck S, Kesharwani S, Seefeldt T, et al. The flavonoid metabolite 2,4,6-trihydroxybenzoic acid is a CDK inhibitor and an anti-proliferative agent: a potential role in cancer prevention. Cancers 2019;11:427.
22. Dickler MN, Tolaney SM, Rugo HS, Cortés J, Diéras V, Patt D, et al. MONARCH 1, a phase II study of abemaciclib, a CDK4 and CDK6 inhibitor, as a single agent, in patients with refractory HR(+)/HER2(-) metastatic breast cancer. Clin Cancer Res 2017;23:5218–24.
23. Finn RS, Crown JP, Lang I, Boer K, Bondarenko IM, Kulyk SO, et al. The cyclin-dependent kinase 4/6 inhibitor palbociclib in combination with letrozole versus letrozole alone as first-line treatment of oestrogen receptor-positive, HER2-negative, advanced breast cancer (PALOMA-1/TRIO-18): a randomised phase 2 study. Lancet Oncol 2015;16:25–35.
24. Hortobagyi GN, Stemmer SM, Burris HA, Yap Y-S, Sonke GS, Paluch-Shimon S, et al. Ribociclib as first-line therapy for HR-positive, advanced breast cancer. N Engl J Med 2016;375:1738–48.
25. Sledge GW, Toi M, Neven P, Sohn J, Inoue K, Pivot X, et al. MONARCH 2: Abemaciclib in combination with fulvestrant in women with HR+/HER2- advanced breast cancer who had progressed while receiving endocrine therapy. J Clin Oncol 2017;35:2875–84.
26. Malumbres M, Harlow E, Hunt T, Hunter T, Lahti JM, Manning G, et al. Cyclin-dependent kinases: a family portrait. Nat Cell Biol 2009;11:1275–6.
27. Fischer PM, Lane DP. Inhibitors of cyclin-dependent kinases as anti-cancer therapeutics. Curr Med Chem 2000;7:1213–45.
28. Peyressatre M, Prevel C, Pellerano M, Morris MC. Targeting cyclin-dependent kinases in human cancers: from small molecules to Peptide inhibitors. Cancers 2015;7:179–237.
29. Morales F, Giordano A. Overview of CDK9 as a target in cancer research. Cell Cycle 2016;15:519–27.
30. Byth KF, Thomas A, Hughes G, Forder C, McGregor A, Geh C, et al. AZD5438, a potent oral inhibitor of cyclin-dependent kinases 1, 2, and 9, leads to pharmacodynamic changes and potent antitumor effects in human tumor xenografts. Mol Cancer Ther 2009;8:1856–66.
31. Cai D, Latham VM Jr, Zhang X, Shapiro GI. Combined depletion of cell cycle and transcriptional cyclin-dependent kinase activities induces apoptosis in cancer cells. Cancer Res 2006;66:9270–80.
32. Payton M, Chung G, Yakowec P, Wong A, Powers D, Xiong L, et al. Discovery and evaluation of dual CDK1 and CDK2 inhibitors. Cancer Res 2006;66:4299–308.
33. Bačević K, Lossaint G, Achour TN, Georget V, Fisher D, Dulić V. Cdk2 strengthens the intra-S checkpoint and counteracts cell cycle exit induced by DNA damage. Sci Rep 2017;7:13429.
34. Jang SH, Kim AR, Park NH, Park JW, Han IS. DRG2 Regulates G_2–M progression via the cyclin B1-Cdk1 complex. Mol Cells 2016;39:699–704.
35. Galimberti F, Thompson SL, Liu X, Li H, Memoli V, Green SR, et al. Targeting the cyclin E-Cdk-2 complex represses lung cancer growth by triggering anaphase catastrophe. Clin Cancer Res 2010;16:109–120.
36. Tentler JJ, Tan AC, Weekes CD, Jimeno A, Leong S, Pitts TM, et al. Patient-derived tumour xenografts as models for oncology drug development. Nat Rev Clin Oncol 2012;9:338–50.
37. Altunel E, Roghani RS, Chen K-Y, Kim SoY, McCall S, Ware KE, et al. Development of a precision medicine pipeline to identify personalized treatments for colorectal cancer. BMC Cancer 2020;20:592.
38. Izumchenko E, Paz K, Ciznadija D, Sloma I, Katz A, Vasquez-Dunddel D, et al. Patient-derived xenografts effectively capture responses to oncology therapy in a heterogeneous cohort of patients with solid tumors. Ann Oncol 2017;28:2595–605.
39. Evrard YA, Srivastava A, Randjelovic J, Doroshow JH, Dean DA, Morris JS, et al. Systematic establishment of robustness and standards in patient-derived xenograft experiments and analysis. Cancer Res 2020;80:2286–97.
40. Ghimessy AK, Gellert A, Schlegl E, Hegedus B, Raso E, Barbai T, et al. KRAS mutations predict response and outcome in advanced lung adenocarcinoma patients receiving first-line bevacizumab and platinum-based chemotherapy. Cancers 2019;11:1514.
41. Suzawa K, Offin M, Lu D, Kurzatkowski C, Vojnic M, Smith RS, et al. Activation of KRAS mediates resistance to targeted therapy in MET Exon 14-mutant non-small cell lung cancer. Clin Cancer Res 2019;25:1248–60.
42. Whittaker SR, Mallinger A, Workman P, Clarke PA. Inhibitors of cyclin-dependent kinases as cancer therapeutics. Pharmacol Ther 2017;173:83–105.
43. Asghar U, Witkiewicz AK, Turner NC, Knudsen ES. The history and future of targeting cyclin-dependent kinases in cancer therapy. Nat Rev Drug Discov 2015; 14:130–46.
44. Chou J, Quigley DA, Robinson TM, Feng FY, Ashworth A. Transcription-associated cyclin-dependent kinases as targets and biomarkers for cancer therapy. Cancer Discov 2020;10:351–70.
45. Shapiro GI, Supko JG, Patterson A, Lynch C, Lucca J, Zacarola PF, et al. A phase II trial of the cyclin-dependent kinase inhibitor flavopiridol in patients with previously untreated stage IV non-small cell lung cancer. Clin Cancer Res 2001;7:1590–9.
46. Stadler WM, Vogelzang NJ, Amato R, Sosman J, Taber D, Liebowitz D, et al. Flavopiridol, a novel cyclin-dependent kinase inhibitor, in metastatic renal cancer: a University of Chicago Phase II Consortium study. J Clin Oncol 2000;18:371–5.
47. Boss DS, Schwartz GK, Middleton MR, Amakye DD, Swaisland H, Midgley RS, et al. Safety, tolerability, pharmacokinetics and pharmacodynamics of the oral cyclin-dependent kinase inhibitor AZD5438 when administered at intermittent and continuous dosing schedules in patients with advanced solid tumours. Ann Oncol 2010;21:884–94.
48. O'Hara MH, Edmonds C, Farwell M, Perini RF, Pryma DA, Teitelbaum UR, et al. Phase II pharmacodynamic trial of palbociclib in patients with KRAS mutant colorectal cancer. J Clin Oncol 2015;33:626.
49. Sedlacek H, Czech J, Naik R, Kaur G, Worland P, Losiewicz M, et al. Flavopiridol (L86 8275; NSC 649890), a new kinase inhibitor for tumor therapy. Int J Oncol 1996;9:1143–68.

50. Aklilu M, Kindler HL, Donehower RC, Mani S, Vokes EE. Phase II study of flavopiridol in patients with advanced colorectal cancer. Ann Oncol 2003;14:1270–3.
51. Pagano M, Pepperkok R, Lukas J, Baldin V, Ansorge W, Bartek J, et al. Regulation of the cell cycle by the cdk2 protein kinase in cultured human fibroblasts. J Cell Biol 1993;121:101–11.
52. Gabrielli BG, Roy LM, Maller JL. Requirement for Cdk2 in cytostatic factor-mediated metaphase II arrest. Science 1993;259:1766–9.
53. Wada T, Takagi T, Yamaguchi Y, Watanabe D, Handa H. Evidence that P-TEFb alleviates the negative effect of DSIF on RNA polymerase II-dependent transcription in vitro. Embo j 1998;17:7395–403.
54. Whittaker SR, Barlow C, Martin MP, Mancusi C, Wagner S, Self A, et al. Molecular profiling and combinatorial activity of CCT068127: a potent CDK2 and CDK9 inhibitor. Mol Oncol 2018;12:287–304.
55. Kawakami M, Mustachio LM, Rodriguez-Canales J, Mino B, Roszik J, Tong P, et al. Next-generation CDK2/9 inhibitors and anaphase catastrophe in lung cancer. J Natl Cancer Inst 2017;109:djw297.
56. Navarro-Serer B, Childers EP, Hermance NM, Mercadante D, Manning AL. Aurora A inhibition limits centrosome clustering and promotes mitotic catastrophe in cells with supernumerary centrosomes. Oncotarget 2019;10:1649–59.
57. Gergely F, Basto R. Multiple centrosomes: together they stand, divided they fall. Genes Dev 2008;22:2291–6.
58. Quintyne NJ, Reing JE, Hoffelder DR, Gollin SM, Saunders WS. Spindle multipolarity is prevented by centrosomal clustering. Science 2005;307:127–9.
59. Kawakami M, Mustachio LM, Liu X, Dmitrovsky E. Engaging anaphase catastrophe mechanisms to eradicate aneuploid cancers. Mol Cancer Ther 2018;17:724–31.
60. Takagi K, Sowa Y, Cevik OM, Nakanishi R, Sakai T. CDK inhibitor enhances the sensitivity to 5-fluorouracil in colorectal cancer cells. Int J Oncol 2008;32:1105–10.
61. Zhang J, Zhou L, Zhao S, Dicker DT, El-Deiry WS. The CDK4/6 inhibitor palbociclib synergizes with irinotecan to promote colorectal cancer cell death under hypoxia. Cell Cycle 2017;16:1193–200.
62. Kalan S, Amat R, Schachter MM, Kwiatkowski N, Abraham BJ, Liang Y, et al. Activation of the p53 transcriptional program sensitizes cancer cells to Cdk7 inhibitors. Cell Rep 2017;21:467–81.
63. Zhang P, Kawakami H, Liu W, Zeng X, Strebhardt K, Tao K, et al. Targeting CDK1 and MEK/ERK overcomes apoptotic resistance in BRAF-mutant human colorectal cancer. Mol Cancer Res 2018;16:378–89.
64. Boj SF, Hwang C-Il, Baker LA, Chio IInC, Engle DD, Corbo V, et al. Organoid models of human and mouse ductal pancreatic cancer. Cell 2015;160:324–38.
65. Gao D, Vela I, Sboner A, Iaquinta PJ, Karthaus WR, Gopalan A, et al. Organoid cultures derived from patients with advanced prostate cancer. Cell 2014;159:176–87.
66. Broutier L, Mastrogiovanni G, Verstegen MMa, Francies HE, Gavarró LM, Bradshaw CR, et al. Human primary liver cancer-derived organoid cultures for disease modeling and drug screening. Nat Med 2017;23:1424–35.
67. Sachs N, de Ligt J, Kopper O, Gogola E, Bounova G, Weeber F, et al. A living biobank of breast cancer organoids captures disease heterogeneity. Cell 2018;172:373–86.
68. Kim M, Mun H, Sung CO, Cho EJ, Jeon H-J, Chun S-M, et al. Patient-derived lung cancer organoids as in vitro cancer models for therapeutic screening. Nat Commun 2019;10:3991.
69. Kondo J, Inoue M. Application of cancer organoid model for drug screening and personalized therapy. Cells 2019;8:470.

Published OnlineFirst November 6, 2020; DOI: 10.1158/1535-7163.MCT-20-0454

Molecular Cancer Therapeutics

A Precision Medicine Drug Discovery Pipeline Identifies Combined CDK2 and 9 Inhibition as a Novel Therapeutic Strategy in Colorectal Cancer

Jason A. Somarelli, Roham Salman Roghani, Ali Sanjari Moghaddam, et al.

Mol Cancer Ther 2020;19:2516-2527. Published OnlineFirst November 6, 2020.